Hindawi Publishing Corporation
Mathematical Problems in Engineering
Volume 2012, Article ID 404073, 15 pages
doi:10.1155/2012/404073

Research Article

Optimal Sizing and Control Strategy Design for Heavy Hybrid Electric Truck

Yuan Zou, Dong-ge Li, and Xiao-song Hu

National Engineering Laboratory for Electric Vehicles, School of Mechanical Engineering, Beijing Institute of Technology, Beijing 100081, China

Correspondence should be addressed to Yuan Zou, zouyuan@bit.edu.cn

Received 6 September 2012; Accepted 28 October 2012

Academic Editor: Huimin Niu

Due to the complexity of the hybrid powertrain, the control is highly involved to improve the collaborations of the different components. For the specific powertrain, the components' sizing just gives the possibility to propel the vehicle and the control will realize the function of the propulsion. Definitely the components' sizing also gives the constraints to the control design, which cause a close coupling between the sizing and control strategy design. This paper presents a parametric study focused on sizing of the powertrain components and optimization of the power split between the engine and electric motor for minimizing the fuel consumption. A framework is put forward to accomplish the optimal sizing and control design for a heavy parallel pre-AMT hybrid truck under the natural driving schedule. The iterative plant-controller combined optimization methodology is adopted to optimize the key parameters of the plant and control strategy simultaneously. A scalable powertrain model based on a bilevel optimization framework is built. Dynamic programming is applied to find the optimal control in the inner loop with a prescribed cycle. The parameters are optimized in the outer loop. The results are analysed and the optimal sizing and control strategy are achieved simultaneously.

1. Introduction

The parallel power-train is one of the most effective configurations for hybrid electric vehicles (HEVs). The benefits of the parallel power-train result from its ability to drive with the engine or the electric motor only, or with both. How to minimize the fuel consumption of this type of HEV is presently quite hot in the academic community. Several energy management strategies have been studied or implemented in the literatures [1–5]. Sciarretta and Guzzella [6] suggested that HEV energy control strategy can be mainly categorized into four groups—the numerical optimization method, the analytic optimization method, the equivalent consumption minimization strategy, and the heuristic strategy. Dynamic

programming (DP) is a numerical method for solving multi-stage decision-making problems and has been widely applied to explore the possible maximum fuel saving for the parallel HEVs [7, 8]. However, an optimal control strategy with the inappropriate component sizing could not guarantee the best fuel economy. It means that component sizing should be studied along with power management strategy to acquire the optimal performance. Hence, the combined optimization problem of the power management and component sizing for HEV is important. The combined plant/controller optimization problem has been researched a lot. For example, [9] discussed several implementations for the combined optimization strategy: the sequential, iterative, bilevel, and simultaneous manners, in which bilevel form was most commonly used [10]. Wu et al. [11, 12] optimized the components' sizes and rule-based control strategy parameters for a hybrid electric vehicle. The highly accurate models were considered in the bilevel framework in [13]. A parameterized powertrain model and the near-optimal controller constituted a combined optimization problem for a fuel cell hybrid vehicle [14]. However, due to the near-optimal controller, the vehicle fuel saving was a bit unsatisfactory. Delphine et al. built a scalable powertrain model to form an integrated optimization problem, in which the outer loop chose the battery capacity, maximum torque of engine and motor as the variables, while dynamic programming was applied to find the optimal control strategy in the inner loop. Each simulation adjusted merely one parameter while keeping the remainder fixed [15]. Therefore, the coupling effects among component parameters were neglected.

In this study, the combined power management and sizing optimization problem for a heavy parallel hybrid electric truck is formulated and solved in a bilevel manner. The paper starts from the power train modelling, including the engine, the motor, the battery, and the transmission. Through the bilevel framework, a scalable vehicle model is developed and integrated in the optimal design process. DP is applied for the power management in the inner loop and the main parameters of the components are optimized simultaneously in the outer loop. The coupling among the component parameters is studied and the considerable fuel economy improvements are achieved.

2. Vehicle Model

2.1. Vehicle Configuration

The baseline vehicle is shown in Figure 1. The hybrid electric truck is a pre-transmission parallel HEV. The engine is connected to an automatic clutch, and then to the transmission. The parameters of this vehicle are given in Table 1.

2.2. Model Simplification

It is highly desirable to perform the extensive simulations for HEVs with the different component configurations at the preliminary system design and optimization. It also means that the scalable model is in great demand at that stage. To avoid the dependence on the specific efficiency maps, a universal representation of the internal combustion engine based on the Willans line concept has been adopted [16]. Considering the complexity of the combined optimization, a simplified scalable motor model is also built later. Those models only consider the dynamic effects related to the low frequency power flows. The transient phenomena, such as chemical reactions in the battery and electric dynamics in the motor, are

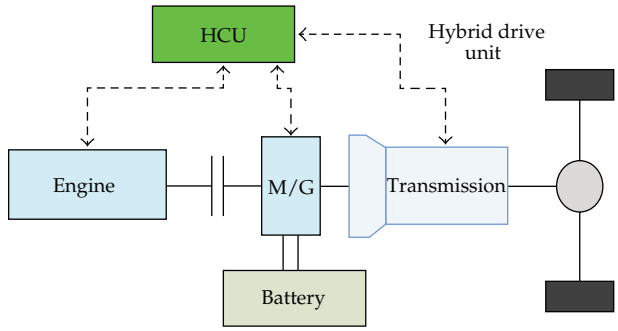

Figure 1: Schematic diagram of the hybrid electric truck.

Table 1: Parameters of the hybrid electric truck.

DI diesel engine	7.0 L, 155 kw@2000 rpm, 900 Nm@1300–1600 rpm
AC motor	Maximum power: 90 kw Maximum torque: 600 Nm Maximum speed: 2400 rpm
Lithium-ion battery	Capacity: 60 Ah Number of modules: 25 Nominal voltage: 12.5 (volts/module)
AMT	9 speed, gear ratio: 12.11/8.08/5.93/4.42/3.36/2.41/1.76/1.32/1
Vehicle	Curb weight: 16000 kg

ignored. Due to the fact that the computation cost increases exponentially as the number of state increases, only the gear number and SOC are chosen to be the system states.

(1) Engine Modeling

The mean effective pressure p_{me} and the mean piston speed c_m are used to describe the engine power and the operating condition. The following three normalizations are used to define the engine efficiency by avoiding the quantities which depends on the engine size [17]:

$$\begin{aligned} p_{\text{me}} &= \frac{4 \cdot \pi}{V_d} \cdot T_e, \\ p_{\text{ma}} &= \frac{4 \cdot \pi \cdot H_{\text{LHV}}}{V_d} \cdot \frac{\dot{m}}{\omega}, \\ c_m &= \frac{S}{\pi} \cdot \omega, \end{aligned} \tag{2.1}$$

where V_d is the engine's displaced volume, S is the stoke, $\dot{m}$ is the fuel mass flow rate, and H_{LHV} is the fuel low heating value. T_e is the engine effective torque, ω is the engine angular

speed, and p_{ma} can be interpreted as an available mean pressure. When the energy converting efficiency is considered, the following exist:

$$\begin{aligned} T_e \cdot \omega_e &= \eta \cdot \dot{m} \cdot H_{\mathrm{LHV}}, \\ T_e = e \cdot T_a - T_{\mathrm{loss}} &= e \cdot \frac{\dot{m} \cdot H_{\mathrm{LHV}}}{\omega} - T_{\mathrm{loss}}, \end{aligned} \tag{2.2}$$

where η is the engine efficiency, e is the thermodynamic efficiency, and T_a is the available torque that would be generated by engine if all the chemical energy were converted into mechanical form. T_{loss} is the inner loss. Associating (2.1) and (2.2), a dimensionless definition of the engine efficiency can be acquired:

$$\begin{aligned} p_{\mathrm{me}} = e \cdot p_{\mathrm{ma}} - p_{m\mathrm{loss}}, \qquad \eta = \frac{p_{\mathrm{me}}}{p_{\mathrm{ma}}}, \\ p_{m\mathrm{loss}} = \frac{4 \cdot \pi}{V_d} \cdot T_{\mathrm{loss}}. \end{aligned} \tag{2.3}$$

The two parameters e and $p_{m\mathrm{loss}}$ are the functions of the engine speed and load. The following parameterizations have been experimentally validated on the different engines [18]:

$$\begin{aligned} e &= e_0(c_m) - e_1(c_m) \cdot p_{\mathrm{ma}}, \\ e_0(c_m) &= e_{00} + e_{01} \cdot c_m + e_{02} \cdot c_m^2, \\ e_1(c_m) &= e_{10} + e_{11} \cdot c_m, \\ p_{m\mathrm{loss}} &= p_{m\mathrm{loss}0} + p_{m\mathrm{loss}2} \cdot c_m^2. \end{aligned} \tag{2.4}$$

The coefficients, $e_{00}, e_{01}, e_{02}, e_{10}, e_{11}$, $p_{m\mathrm{loss}0}$, and $p_{m\mathrm{loss}2}$, remain unchanged for the different engines in the same family and are obtained through the bench test and parameter identification. Hence the actual engine behavior from the same family is defined by the two size parameters, the swept volume V_d and the piston stroke S. Figure 2 compares the engine model with the actual data collected from the bench experiments for a prototype 7.0 L compression-ignition engine.

(2) Motor Modeling

The motor is modeled based on the experimental data. The motor efficiency is considered as a constant because of its high average efficiency in its feasible working area. Due to the battery power and the motor torque limits, the final motor torque becomes

$$T_m = \begin{cases} \min\left(T_{m,\mathrm{req}}, T_{m,\mathrm{dis}}(\omega_m), T_{\mathrm{bat,dis}}(\mathrm{SOC}, \omega_m)\right), & \text{if } T_{m,\mathrm{req}} > 0, \\ \max\left(T_{m,\mathrm{req}}, T_{m,\mathrm{chg}}(\omega_m), T_{\mathrm{bat,chg}}(\mathrm{SOC}, \omega_m)\right), & \text{if } T_{m,\mathrm{req}} < 0, \end{cases} \tag{2.5}$$

where $T_{m,\mathrm{req}}$ is the requested motor torque. $T_{m,\mathrm{dis}}(\omega_m)$ and $T_{m,\mathrm{chg}}(\omega_m)$ are the maximum motor torques in the motoring and charging modes, respectively. $T_{\mathrm{bat,dis}}(\mathrm{SOC}, \omega_m)$

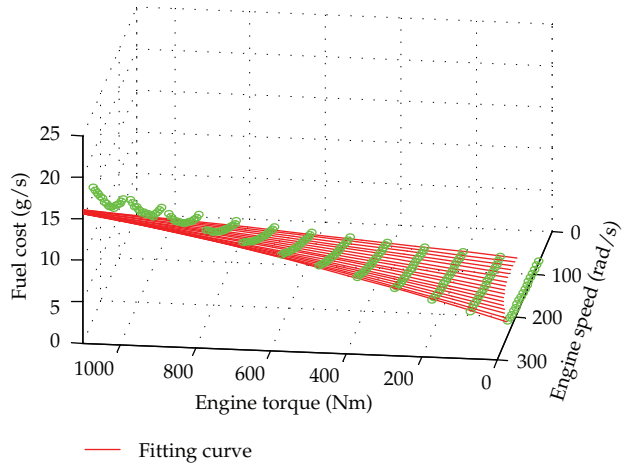

Figure 2: The comparison of Willans line model with the test data of the engine.

and $T_{\text{bat,chg}}(\text{SOC}, \omega_m)$ are the torque bounds due to the battery current limits in the discharging and charging modes.

(3) Battery Modeling

The thermal-temperature effects and transients are ignored. SOC is calculated by

$$\text{SOC}(k+1) = \text{SOC}(k) - \frac{V_{\text{oc}} - \sqrt{V_{\text{oc}}^2 - 4(R_{\text{int}} + R_t) \cdot T_m \cdot \omega_m \cdot \eta_m^{-\text{sgn}(T_m)}}}{2(R_{\text{int}} + R_t) \cdot C_b}, \tag{2.6}$$

where the internal resistance R_{int} and the open circuit voltage V_{oc} are functions of the battery SOC, obtained through the bench test. C_b is the maximum battery charge, R_t is the terminal resistance, and η_m is the efficiency of the motor.

(4) Driveline Modeling

The driveline is defined as the system from the transmission input shaft to wheels. Assuming perfect clutches and gear shifting, the following equations describe the transmission and final drive gear models:

$$\begin{aligned} T_{\text{wheel}} &= \eta_{\text{gear}} \cdot \eta_{\text{FD}} \cdot i_g \cdot i_0 \cdot T_i - \eta_t \cdot \omega_i, \\ \omega_i &= i_g \cdot i_0 \cdot \omega_{\text{wheel}}, \end{aligned} \tag{2.7}$$

where i_g is the transmission gear ratio, i_0 is the final drive gear ratio, η_{gear} and η_{FD} are the transmission and final drive efficiency, respectively. T_i and T_{wheel} are the transmission input torque and output torque, respectively. η_t is the transmission viscous-loss coefficient, ω_i is the transmission input speed, and ω_{wheel} is the wheel speed.

The gear-shifting sequence of the AMT is modeled as a discrete dynamic system:

$$\text{gear}(k+1) = \begin{cases} 9, & \text{gear}(k) + \text{shift}(k) > 9 \\ 1, & \text{gear}(k) + \text{shift}(k) < 1 \\ \text{gear}(k) + \text{shift}(k), & \text{otherwise}, \end{cases} \tag{2.8}$$

where the state $\text{gear}(k)$ is the gear number, and the control $\text{shift}(k)$ to the transmission is constrained to take on the values of -1, 0, and 1, representing down shifting, sustaining, and upshifting, respectively.

(5) Vehicle Dynamics

It is a common practice that only the vehicle longitudinal dynamics is considered. The longitudinal vehicle dynamics is modeled as a point-mass:

$$\omega_{\text{wheel}}(k+1) = \omega_{\text{wheel}}(k) + \frac{T_{\text{wheel}} - T_{\text{brake}} - r_\omega \cdot (F_r + F_a)}{M_r \cdot r_\omega^2}, \tag{2.9}$$

where T_{brake} is the friction brake torque, F_r and F_a are the rolling resistance force, and the aerodynamic drag force, and r_ω is the dynamic tire radius. $M_r = M_V + J_r/r_\omega^2$ is the effective mass of the vehicle, and J_r is the equivalent inertia of the rotating components in the vehicle.

3. Combined Optimization Problem Formulation

3.1. Combined Optimization Framework

Given the particular system parameters, DP can be used to find the optimal control theoretically subject to some constraints under a specific driving schedule. When the system parameters vary in the feasible scope, DP is iteratively applied. The optimal combination of the parameters and control will be identified simultaneously. The bilevel combined plant/controller optimization is adopted, consisting of two nested optimization loops. The outer loop evaluates the system parameters. The inner loop generates the optimal control strategy for the parameters selected by the outer loop. These two loops form the integrated plant/controller optimization, which guarantees the global optimal design for the system parameters and control strategy. The combined optimization problem is complicated, due to the interaction between system parameters and control optimization, and computationally expensive due to the bilevel iterative search process. In order to improve the computational efficiency, once the constraints in the inner loop are violated, the current search stops, and the current cost will be set to a huge infeasible value. The flow chart of the bilevel combined optimization process is shown in Figure 3.

3.2. The Scaled Model and Optimization Problem Formulation

The scaled models are needed to parameterize the system conveniently in the optimization. The scope of the motor torque, the motor speed, the motor power, the engine volume, the cylinder stoke, the battery numbers, and the capacity of battery are scaled by mot_tor,

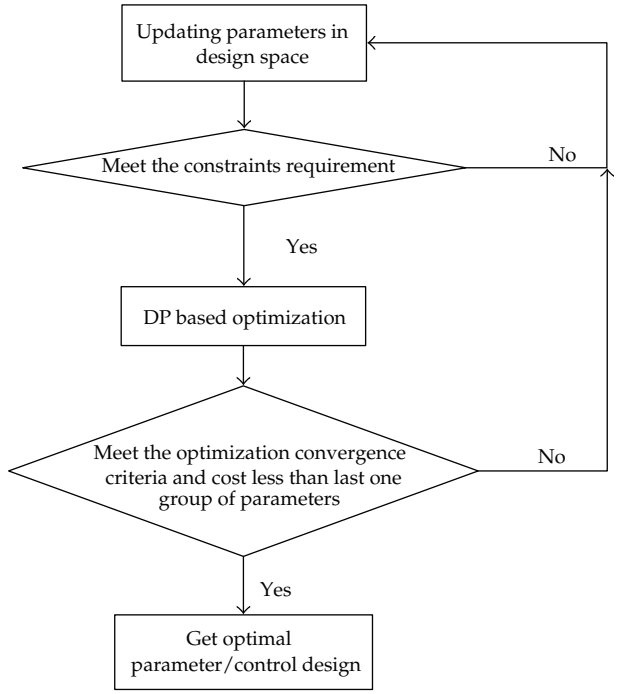

Figure 3: The bilevel combined optimization process.

mot_spd, motorp, Vdscale, Sscale, bat_num, and bat_ah,respectively. The final drive ratio i_0, varying within a certain range without a scale enlarging, is one of the design parameters. The component parameters are described as follows:

$$\begin{aligned}
C_b &= \text{bat_ah} \cdot C_{b_\text{bas}}, \\
V_{\text{oc}} &= \text{bat_num} \cdot \text{Nbas} \cdot V_{\text{oc_bas}}, \\
V_d &= V_{d_\text{bas}} \cdot Vd\text{scale}, \\
S &= S\text{scale} \cdot S_{\text{bas}}, \\
Mt &= \text{mot_tor} \cdot Mt_{\text{bas}}, \\
Ms &= \text{mot_spd} \cdot Ms_{\text{bas}}, \\
Mp &= \text{motorp} \cdot Mp_{\text{bas}}, \\
R_{\text{int}} &= \frac{\text{bat_num}}{\text{bat_ah}} \cdot R_{\text{int_bas}}, \\
R_t &= \frac{\text{bat_num}}{\text{bat_ah}} \cdot R_{t_\text{bas}},
\end{aligned} \tag{3.1}$$

where C_{b_bas} and Nbas are the baseline battery capacity and the baseline number of the battery pack, $V_{\text{oc\_bas}}$ is the baseline open circuit voltage of battery pack as a function of SOC. $R_{\text{int\_bas}}$

and R_{t_bas} are the baseline internal resistance and terminal resistance. Mt_{bas}, Ms_{bas}, and Mp_{bas} are the baseline parameters of the motor, while $V_{d\mathrm{bas}}$ and S_{bas} are those of the engine. The baseline parameters are listed in Table 1. The variables in the left hand of the equations are the scaled parameters that need to be transferred to the inner loop.

The degree of hybridization (DOH) is often adopted to measure the relative contributions of the primary and second power sources. As to the parallel hybrid electric vehicles, the engine is often the primary power source and the battery the secondary power source. The DOH is constrained to be within [0, 0.4] and calculated by

$$x_h = \frac{P_{m\_\max}}{P_{e\_\max} + P_{m\_\max}}, \tag{3.2}$$

where $P_{m\_\max}$ is the maximum power that the motor offers, and $P_{e\_\max}$ is the maximum power that the engine provides. The combined optimal problem is formulated with all the constraints by

$$\min_{\substack{\text{mot\_tor, mot\_spd, bat\_num,}\\ \text{bat\_ah, } i_0\text{, motorp, } S\text{scale, } Vd\text{scale}}} \left\{ \sum_{i=0}^{N-1} T_s \cdot F_d\left(n_{\mathrm{eng}}(k), T_{\mathrm{eng}}(K)\right) \right\} \tag{3.3}$$

subject to

$$\begin{gathered} x(k+1) = f(x(k), u(k)), \\ 0.3 \le \text{mot\_tor} \le 2, \\ 0.9 \le \text{mot\_spd} \le 2, \\ 0.5 \le \text{motorp} \le 1.5, \\ 0.7 \le Vd\text{scale} \le 1.5, \\ 0.9 \le S\text{scale} \le 1.2, \\ 0.5 \le \text{bat\_num} \le 3, \\ 0.5 \le \text{bat\_ah} \le 3, \\ 2 \le i_0 \le 8, \\ 0 < x_h \le 0.4, \\ \text{max speed} \ge 50\,\text{mph}, \\ \text{acceleration time } (0 - 50\,\text{mph}) \le 45\,\text{sec}, \\ \text{grade } (\text{at the speed of } 6\,\text{mph}) \ge 20\%, \end{gathered} \tag{3.4}$$

where f represents the dynamics (2.1)–(2.9). The dynamic performance should be limited in the constraints when both the engine and motor propel the car. The constraints on the scaled parameters constitute the design space of the component sizing optimization.

4. Algorithms and Methods

Design of experiments (DOE) technique is first applied to explore the response map in all the feasible design space based on Optimal Latin Hypercube sampling. Then the Nonlinear Programming by Quadratic Lagrangian (NLPQL) algorithm is applied to obtain the global optimal solution [19]. The group of parameters derived from DOE is optimal among the randomly selected points and will be the initial design point for NLPQL algorithm which can build a quadratic approximation. The quadratic programming problem is iteratively solved to find an improved solution until the final convergence to the optimum design.

Dynamic Programming (DP) is a powerful tool for solving optimization problems due to its guaranteed global optimality even for nonlinear dynamic systems with constraints. For a given driving cycle, DP can obtain the optimal operating strategy minimizing fuel consumption.

For maximizing the fuel saving of HEV, the cost function to be minimized has the following form:

$$J = \sum_{k=0}^{N-1} \left[L_{\text{fuel}}(k) + \beta \cdot |\text{shift}(k)| \right] + G_N(x_{\text{SOC}}(N)), \tag{4.1}$$

where $L_{\text{fuel}}(k)$ is the instantaneous cost of the fuel use. The vehicle drivability is constrained by $\beta \cdot |\text{shift}(k)|$ to avoid excessive shifting, in which β is a positive weighting factor. A terminal constraint on SOC, represented by $G_N(x_{\text{SOC}}(N))$, is imposed on the cost function due to the charge-sustaining strategy. During the optimization, it is necessary to enforce the following inequality constraints to ensure safe and smooth operation for the engine, the battery, and the motor:

$$\begin{gathered} \omega_{e\_\min} \le \omega_e(k) \le \omega_{e\_\max}, \\ \text{SOC}_{\min} \le \text{SOC}(k) \le \text{SOC}_{\max}, \\ T_{e\_\min}(\omega_e(k)) \le T_e(k) \le T_{e\_\max}(\omega_e(k)), \\ T_{m\_\min}(\omega_e(k), \text{SOC}(k)) \le T_m(k) \le T_{m\_\max}(\omega_e(k), \text{SOC}(k)), \end{gathered} \tag{4.2}$$

where ω_e is the engine speed, SOC is the battery state of charge. $\text{SOC}_{\min}$ and $\text{SOC}_{\max}$ are selected to be 0.4 and 0.8, respectively. T_e is the engine torque, and T_m is the motor torque. A generic DP algorithm is implemented in MATLAB and applied to solve the above optimal control problem [20, 21].

5. Simulations and Results

The heavy-duty vehicle driving schedule used to evaluate the fuel economy of the hybrid electric truck is shown in Figure 4.

The Pareto figure indicating the influence of the various factors on the fuel consumption is shown in Figure 5. It is determined by ordering the scaled and normalized coefficients of a standard least-squares second-order polynomial fit to the contribution to the fuel consumption from the different parameters. It is evident that motorp, *vd*scale, and i_0 individually have a significant effect on the fuel consumption. These three parameters

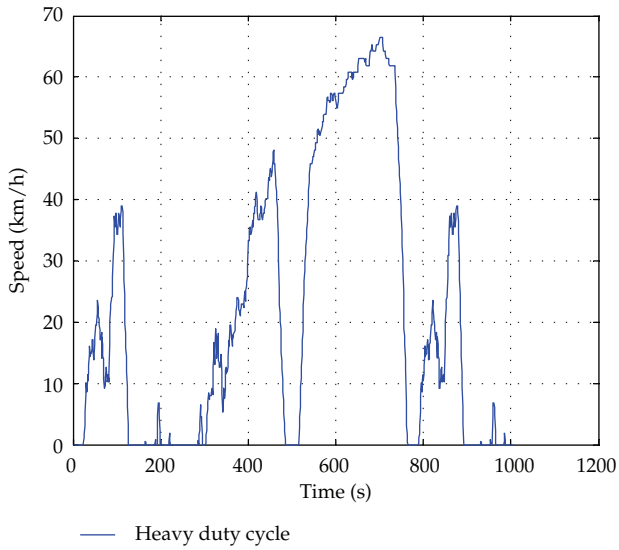

Figure 4: The heavy-duty vehicle driving schedule.

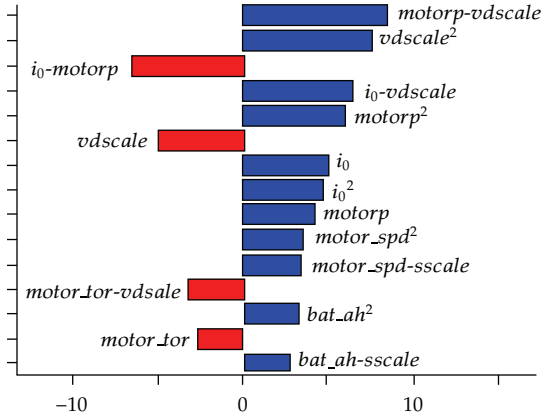

Figure 5: The Pareto plot for the various factors' influence on the fuel consumption.

represent the motor's maximum power, the engine's maximum power, and the final drive ratio, respectively. However, the interaction between the maximum motor power and the engine volume has the largest impact on the fuel consumption. The effects of the battery capacity on the fuel consumption are not as significant as other parameters; the percentage is less than 3%. Therefore, the battery supplying enough power for the motor can be chosen based on the cost effectiveness.

The specific influences on the fuel economy from the power sizing of the engine and the motor are shown in Figure 6. Note that alteration of the engine volume brings the change of the engine maximum power. It can also be concluded that the fuel consumption does not decrease as the engine size reduces or the motor size increases. Both of them should be chosen within a specific range in order to obtain the impressive fuel economy.

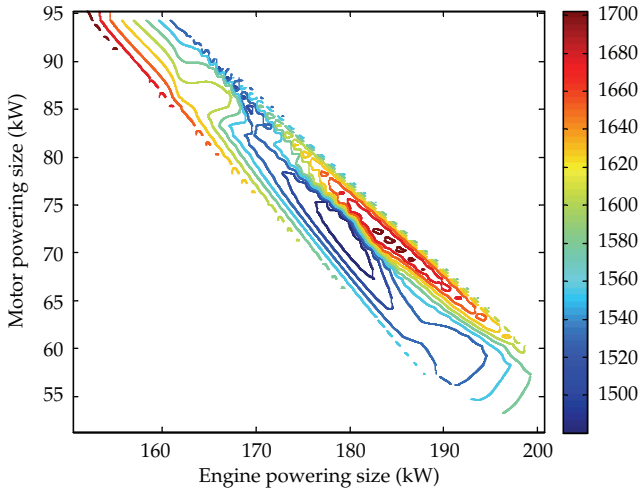

Figure 6: The fuel consumption versus the motor and engine powering size.

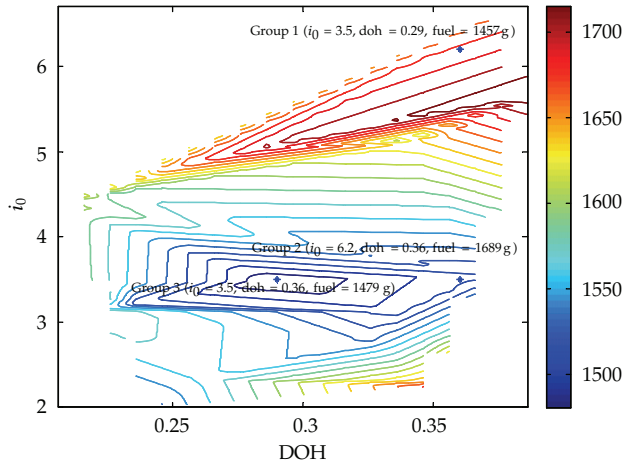

Figure 7: The fuel consumption versus i_0 and DOH.

The parameters of the three typical groups with the different components' sizes are listed in Table 2. The second and third group only differs in the final drive ratio and the third one has the same final ratio with the first one. The three groups of parameters are marked in Figure 7. It may allow the conclusion that the final drive ratio i_0 should be selected within a limited range, roughly between 3 and 4, slightly smaller than the initial value, to keep the good fuel economy, regardless of the DOH. The improper selection of the final drive ratio can lead to the increasing fuel consumption despite the optimal control strategy.

The engine working area and the gear shifting of the first and second group is shown in Figures 8, 9, 10, and 11. The second group with a smaller engine has a fundamentally different gear shifting from the first one. It is easy to extract the shifting rule from Figure 9, whereas difficult to obtain a shifting line for the second group because there is no apparent boundary between neighboring gears in Figure 11. The improper selection of the final drive

Table 2: The comparison within the different groups.

Group number	bat_ah	bat_num	i_0	motor_spd	motor_tor	motorp
1	0.98	0.7	3.50	1.15	1.93	0.77
2	2.59	0.82	6.20	1.55	1.44	1.00
3	2.59	0.82	3.50	1.55	1.44	1.00
Group number	*s*scale	*vd*scale	DOH	Engine's max power (kW)	Total power (kW)	Fuel consumption (g)
1	0.94	1.16	0.29	179	252	1457
2	0.9	1.00	0.36	154	248	1689
3	0.9	1.00	0.36	154	248	1479

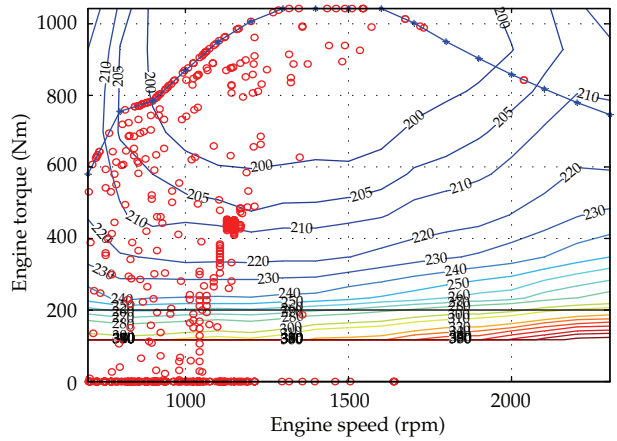

Figure 8: The working area of engine in the first group.

ratio will result in low efficiency working area for the engine more possibly and could not be compensated by optimizing gear shifting and power distribution.

It is clear that the component parameters can affect HEV fuel economy directly. Sometimes a slight parameter discrepancy may lead to the considerable change of the fuel consumption. It emphasizes that the component sizing of HEV should be designed with a great cautiousness.

The optimal and initial parameters are listed in Table 3. The battery capacity decreases to 30 Ah from the original value, 60 Ah, although its voltage increases a bit. The final ratio decreases to 3.3 from the original value 4.769. Although the motor power is decreased, the motor max torque is found to increase by 63% to meet the performance constraints. Around 9% improvement is observed in the fuel economy through the combined optimization. The feasibility of the components in the actual engineering applications, however, needs more investigation in the view of the reliability and cost effectiveness.

6. Conclusion

A bilevel optimization problem for the combined component sizing and power distribution of a heavy hybrid electric truck is formulated and solved. DOE and NPQRL algorithms are

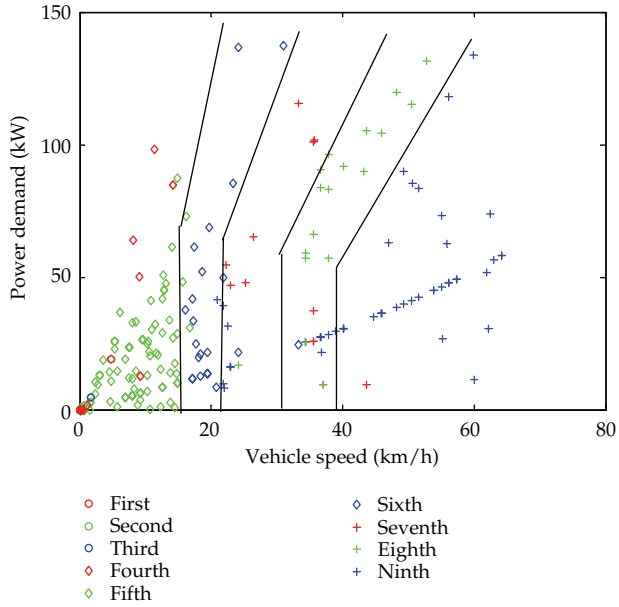

Figure 9: The gear shifting in the first group.

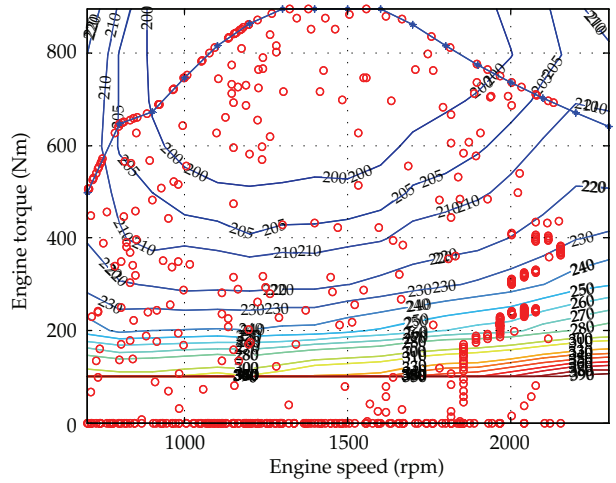

Figure 10: The working area of the engine in the second group.

Table 3: The values of the baseline and optimization parameters.

C (Ah)	V (V)	i_0	Max motor speed (rpm)	Max motor torque (nm)	Max motor power (kW)	Max engine power (kW)	Fuel economy (mile/gallon)
The initial values							
60	312	4.769	2400	600	94	155	26.4
The optimal values							
30	393	3.3	2400	980	83	163	28.7

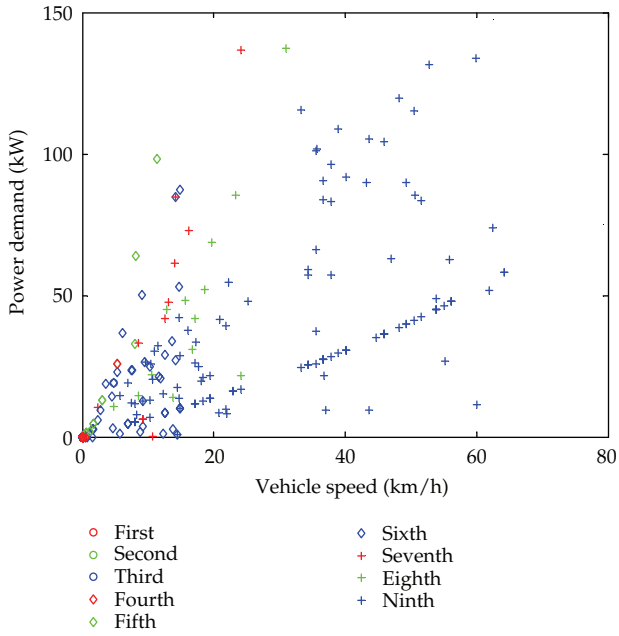

Figure 11: The gear shifting in the second group.

applied to find the optimal component parameters in the outer loop, while DP is used to find the optimal energy strategy in the inner loop. Simulation results show that the complex relationships between the component sizes and fuel consumption can be efficiently analyzed by solving the combined optimization problem. The law extracted from the optimization results can provide the suggestions for the actual hybrid vehicle system optimization and control. The results also indicate that the comprehensive bilevel optimization framework can facilitate the enhancement of HEV fuel economy, and the components sizing is as important as the control strategy.

Acknowledgments

This research is financially supported by China Natural Science Funding Project (50905015), China 863 High Technology Project (2011AA11A223), and China University Discipline Talent Introduction Program (B12022).

References

[1] X. Wei, L. Guzzella, V. I. Utkin, and G. Rizzoni, "Model-based fuel optimal control of hybrid electric vehicle using variable structure control systems," *Journal of Dynamic Systems, Measurement and Control*, vol. 129, no. 1, pp. 13–19, 2007.

[2] A. Sciarretta, M. Back, and L. Guzzella, "Optimal control of parallel hybrid electric vehicles," *IEEE Transactions on Control Systems Technology*, vol. 12, no. 3, pp. 352–363, 2004.

[3] C. C. Lin, M. J. Kim, H. Peng, and J. W. Grizzle, "System-level model and stochastic optimal control for a PEM fuel cell hybrid vehicle," *Journal of Dynamic Systems, Measurement and Control*, vol. 128, no. 4, pp. 878–890, 2006.

[4] S. E. Lyshevski, "Energy conversion and optimal energy management in diesel-electric drivetrains of hybrid-electric vehicles," *Energy Conversion and Management*, vol. 41, no. 1, pp. 13–24, 2000.

[5] C.-C. Lin, H. Peng, J. W. Grizzle, and J. M. Kang, "Power management strategy for a parallel hybrid electric truck," *IEEE Transactions on Control Systems Technology*, vol. 11, no. 6, pp. 839–849, 2003.

[6] A. Sciarretta and L. Guzzella, "Control of hybrid electric vehicles," *IEEE Control Systems Magazine*, vol. 27, no. 2, pp. 60–70, 2007.

[7] B. Gu, *Supervisory control stategy development for a hybrid electric vehicle [M.S. thesis]*, The Ohio State University, Columbus, Ohio, USA, 2006.

[8] L. V. Pérez, G. R. Bossio, D. Moitre, and G. O. García, "Optimization of power management in an hybrid electric vehicle using dynamic programming," *Mathematics and Computers in Simulation*, vol. 73, no. 1–4, pp. 244–254, 2006.

[9] H. K. Fathy, J. A. Reyer, P. Y. Papalambros, and A. G. Ulsoy, "On the coupling between the plant and controller optimization problems," in *Proceedings of the American Control Conference*, pp. 1864–1869, Arlington, Va, USA, June 2001.

[10] J. F. Bonnans, Th. Guilbaud, A. Ketfi-Cherif, C. Sagastizabal, D. Wissel, and H. Zidani, "Parametric optimization of hybrid car engines," *Optimization and Engineering*, vol. 5, no. 4, pp. 395–415, 2004.

[11] J. Wu, C.-H. Zhang, and N.-X. Cui, "Psoalgprithm-based parameter optimizationfor HEV power-train and its control strategy," *International Journal of Automotive Technology*, vol. 9, no. 1, pp. 53–69, 2008.

[12] C. Desai and S. S. Williamson, "Optimal design of a parallel hybrid electric vehicle using multi-objective genetic algorithms," in *Proceedings of the 5th IEEE Vehicle Power and Propulsion Conference (VPPC '09)*, pp. 871–876, Dearborn, Mich, USA, September 2009.

[13] D. Assanis, G. Delagrammatikas, R. Fellini et al., "Optimization approach to hybrid electric propulsion system design," *Mechanics of Structures and Machines*, vol. 27, no. 4, pp. 393–421, 1999.

[14] M.-J. Kim and H. Peng, "Power management and design optimization of fuel cell/battery hybrid vehicles," *Journal of Power Sources*, vol. 165, no. 2, pp. 819–832, 2007.

[15] D. Sinoquet, G. Rousseau, and Y. Milhau, "Design optimization and optimal control for hybrid vehicles," *Optimization and Engineering*, vol. 12, no. 1-2, pp. 199–213, 2011.

[16] X. Wei and G. Rizzoni, "A scalable approach for energy converter modeling and supervisory control design," in *Proceedings of the ASME International Mechanical Engineering Congress and Exposition*, pp. 1281–1288, November 2001.

[17] G. Rizzoni, L. Guzzella, and B. M. Baumann, "Unified modeling of hybrid electric vehicle drivetrains," *IEEE/ASME Transactions on Mechatronics*, vol. 4, no. 3, pp. 246–257, 1999.

[18] A. Urlaub, *Verbrennungsmotoren*, Springer-Verlag, Berlin, Germany, 1994.

[19] Dassault Company, *Isight User Guide (4.5 Release)*, Dassault Company, Velizy-Villacoublay, France, 2010.

[20] Y. Zou, F. Sun, C. Zhang, and J. Li, "Optimal energy management strategy for hybrid electric tracked vehicles," *International Journal of Vehicle Design*, vol. 58, no. 2–4, pp. 307–324, 2012.

[21] O. Sundström and L. Guzzella, "A generic dynamic programming Matlab function," in *Proceedings of the IEEE International Conference on Control Applications (CCA '09)*, pp. 1625–1630, July 2009.